J. Anat. (1987), **150**, pp. 229–245
With 10 *figures*
Printed in Great Britain

The morphology and morphometry of the adult normal baboon lung (*Papio anubis*)

J. N. MAINA

Department of Veterinary Anatomy, University of Nairobi, P.O. Box 30197, *Nairobi, Kenya*

(*Accepted* 18 *March* 1986)

INTRODUCTION

Numerous morphological studies on diverse aspects of the organisation of the mammalian lung notably in respect to structure, development, response to irritants and functional demands are currently available. Some of the most recent accounts and reviews on these aspects are those by Weibel (1973, 1984), Sorokin & Brain (1975), Breeze & Wheeldon (1977), Weibel & Gil (1977), Grant, Sorokin & Brain (1979), Pinkerton *et al.* (1982), Thurlbeck (1982), Hirai, Uyeda & Ogawa (1984), Gehr (1984), Brown, Bliss & Longmore (1984), Lechner (1985), Maina (1985), Burri (1985) and Winkler & Cheville (1985). Recently the lungs of the non-human primates have received special interest (Carstens & Allen, 1969; Kapanci, Weibel, Kaplan & Robinson, 1969; Kaplan, Robinson, Kapanci & Weibel, 1969; Davies & Reid, 1970; Wang & Thurlbeck, 1970; Greenwood & Holland, 1973; Castleman, Dungworth & Tyler, 1975; Kerr & Helmuth, 1974; Kerr, Couture & Allen, 1975; Boyden, 1977; Hislop, Howard & Fairweather, 1984; Wilson, Plopper & Hyde, 1984; Tyler & Plopper, 1985). This is largely due to the notion that the non-human primates, when compared with the other mammalian experimental animals, constitute in most biological aspects a better model for the study of human pulmonary structure, function and pathology (Lapin, 1971; Bourne, 1973). Morphometric methods are particularly effective in studying and evaluating the organisation of the biological tissues as they are sensitive enough to reveal remarkably small structural and developmental changes which otherwise would go undetected by qualitative observations. These techniques have been applied to the lungs of the non-human primates by Kapanci *et al.* (1969), Kaplan *et al.* (1969), Conradi *et al.* (1971) and Hislop *et al.* (1984) to evaluate developmental and experimental situations such as breathing pure oxygen and inhalation of beryllium. As observed by Castleman *et al.* (1975), studies of the tissues of the non-human primates, in view of their potential utilisation in human biological investigations, are few in number. For example, the most extensive morphometric studies illustrating the structure and the gas exchange potential of the primate lung are apparently those on the human lung by Gehr, Bachofen & Weibel (1978) and the macaque monkey (*Macaca irus*) by Conradi *et al.* (1971).

The present study examines the lung of the olive baboon (*Papio anubis*) in an attempt to find out whether its pulmonary organisation is any different from that of the lungs of the other non-human primates and man. The gas exchange structural characteristics of the baboon lung are compared with those of the other primates as far as available data allow.

MATERIALS AND METHODS

The lungs of 4 adult olive baboons (*Papio anubis*), caught during a game-culling exercise by the Kenyan Ministry of Tourism and Wildlife, were killed by intravenous injection with Euthatal (MB[R]) and weighed. The trachea was immediately exposed and a cannula fixed in place after tracheostomy. The diaphragm was exposed caudal to the xiphisternum and carefully punctured on both sides of the mediastinum to cause a pneumothorax. With the animal in a supine position, the lungs were fixed by intratracheal instillation with 2·5 % glutaraldehyde buffered in sodium phosphate, total osmolarity 350 mOsm and pH 7·4 at a pressure head of 25 cm of water. After the fixative had stopped flowing a ligature was placed at the tracheal bifurcation. The lungs, the heart and adhering connective tissue were carefully removed from the thoracic cavity and immersed in fixative for about two weeks after which the heart and the connective tissues were dissected away and the volume of the lungs estimated by the water displacement method.

Transverse slices were cut across the middle of each of the lobes of the lung and the slice placed on a bench and divided into equal cubes which were processed for light microscopy by standard laboratory techniques. The first technically adequate section from each block was stained with haematoxylin and eosin. The volume densities of the parenchyma and the non-parenchyma were estimated by point-counting, field by field, at a magnification of $\times 100$ using a 100-point Zeiss integrating graticule mounted in an eyepiece. The parts of the lobes remaining after taking samples for light microscopy were cut into small cubes about 0·5 cm^3 and laid out on quadratic lattice acetate paper with numbered squares. Four of the cubes from each lobe were picked using randomly generated numbers from a Texas Instruments (TI 58) electronic calculator. The test cubes were diced to small pieces about 2 mm^3 which were separately processed for electron microscopy. This entailed postfixation in 2 % osmium tetroxide for about 2 hours, block staining in uranyl acetate with maleic acid, followed by dehydration in graded concentrations of ethanol starting at 50 % and progressing to absolute ethanol and propylene oxide before infiltration and embedding about five pieces from each part in Epon. One block picked at random from the group was trimmed to eliminate non-parenchymatous components and ultrathin sections were cut, counterstained with lead citrate and examined on a Zeiss EM 10 electron microscope. A maximum of five electron micrographs was taken at an initial magnification of $\times 1900$ from predetermined corners of the 300-wire mesh grids to avoid bias. Where the test corner fell entirely onto an alveolar lumina, this was recorded, and such blanks substituted in the final calculation. The negatives were enlarged by a factor of 3·5 and printed with a superimposed simple square lattice test system (A-100) of Weibel (1979). For each specimen a maximum of 140 micrographs was analysed at a final magnification of $\times 6700$, which was just enough for the components of the parenchyma to be resolved while giving a maximum test area.

The volume densities of the components of the parenchyma, the alveoli, the blood capillaries and the tissue of the interalveolar septa were estimated by point-counting and absolute values calculated from the volume of the parenchyma. The surface areas of the alveoli, capillary endothelium and the red blood cells were estimated by intersection counting. These stereological methods have been extensively described by Weibel (1979). The harmonic mean thicknesses of the blood–gas (tissue) barrier and the plasma layer were estimated by intercept length measurement and the

arithmetic mean thickness of the tissue barrier was estimated using point and intersection counting with a 21, 2 cm long random short line test grid (Weibel & Knight, 1964). The diffusing capacities of the tissue barrier (D_{to_2}) and that of the plasma layer (D_{po_2}) were estimated from their respective surface areas, harmonic mean thicknesses and the oxygen permeation constants. The diffusing capacity of the red blood cell (D_{eo_2}) was calculated from the pulmonary capillary blood volume and the oxygen uptake coefficient of whole blood (θ_{o_2}), adopting the average mammalian venous haematocrit of 45 %. The membrane (D_{mo_2}) and the total morphometric pulmonary diffusing capacity (DL_{o_2}) were subsequently calculated. The model applied is essentially that advanced by Weibel (1970/71) and subsequently extensively applied to the mammalian lung (Gehr *et al.* 1981).

In one of the specimens the accessory lobe was removed and latex rubber (Latex white, ZCP-652-OIOR-Griffin and George Ltd, UK) injected through the lobar bronchus which was then ligated and the latex allowed to set for 24 hours before corrosion in concentrated hydrochloric acid. The cast was cut into small pieces which together with similar pieces of the fresh lung tissue (remaining after taking samples for light microscopy and transmission electron microscopy) were subjected to critical-point drying with liquid carbon dioxide, sputtered with gold-palladium complex and attached to metal chucks for viewing on a Philips PSEM 275 scanning electron microscope.

RESULTS

The baboon pulmonary system consisted of a left and right lung. The left lung was made up of a cranial (apical) lobe, a middle lobe and a caudal (diaphragmatic) lobe. The right lung consisted of cranial, middle, caudal and accessory lobes. The trachea bifurcated to give rise to the left and right principal bronchi which on entering the lung at the hilum divided into the lobar bronchi. Grossly and histologically the lung could be divided into the parenchyma, which mainly consisted of the alveoli, blood capillaries and the tissue of the interalveolar septum, and the non-parenchyma which comprised the large air conducting passages like the bronchi, and the bronchioles, the large blood vessels and connective tissue elements such as lobar septae and the pleura. The interalveolar septa separated adjacent alveoli and were frequently perforated by interalveolar pores, the pores of Kohn (Figs. 1, 9, 10).

The alveolar surface was largely made up of two populations of cells, the more numerous Type II pneumocytes – the granular or cuboidal pneumocytes – and the Type I pneumocytes – the smooth or squamous pneumocytes (Figs. 2, 9, 10). The Type II cells exhibited numerous microvilli on their free borders (Figs. 3, 9, 10) and contained a centrally placed nucleus. The cytoplasm contained numerous organelles such as mitochondria, Golgi apparatus, smooth and rough endoplasmic reticulum and abundant microvesicular bodies, all these features showing the granular pneumocyte to be an active secretory cell. Osmiophilic lamellated bodies (Figs. 3, 4) characterised the Type II cell. Some of these bodies appeared vacuolated, presumably because of the dissolving of their phospholipid material by the fat solvents during tissue processing. Although the Type II cells were more numerous than the Type I cells, they covered only a small part of the alveolar surface as shown by the extent of the intercellular junctions in Figures 9 and 10. The Type I pneumocytes had a centrally placed nucleus with dispersed chromatin material and long cytoplasmic flanges. Most of the organelles such as mitochondria and the Golgi apparatus were found in the perinuclear region. The cytoplasmic arborisation was remarkably

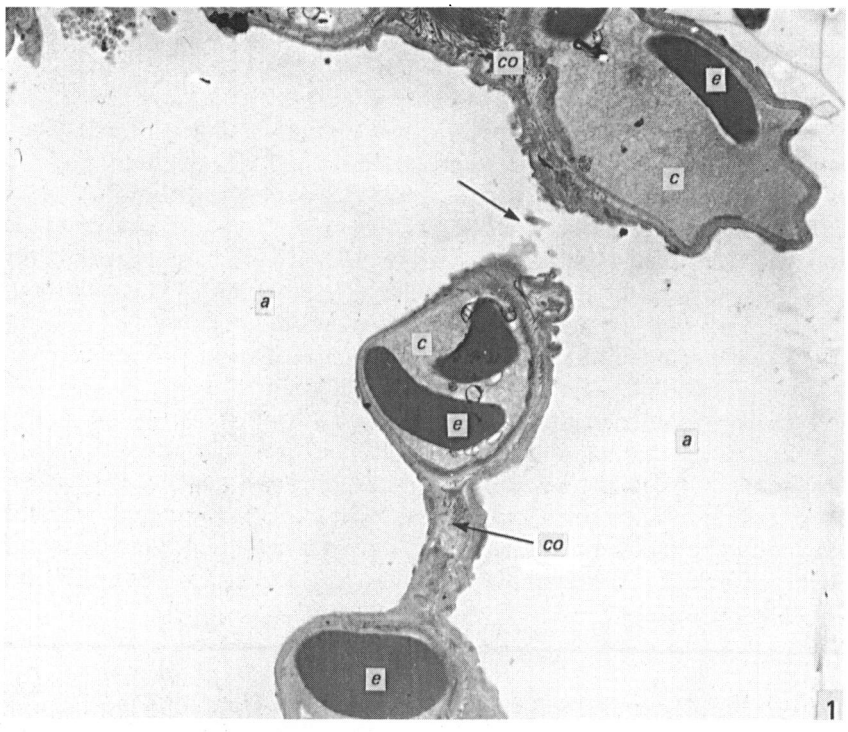

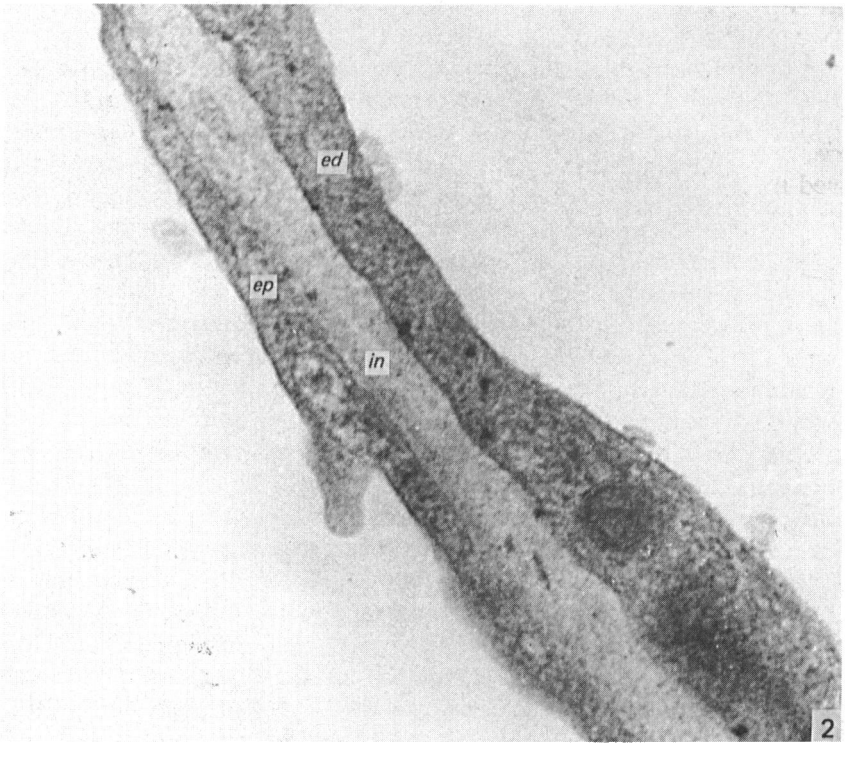

Figs. 1–2. Electron micrographs showing (Fig. 1) the interalveolar septum separating adjacent alveoli. Figure 2 is a high power view of the blood–gas barrier. *c*, blood capillary; *a*, alveolus; *e*, erythrocyte; *ed*, endothelial cell; *co*, collagen; *ep*, epithelial cell; *in*, interstitium. The arrow in Figure 1 shows an interalveolar pore (pore of Kohn). Figure 1 ×4100; Figure 2 ×108000.

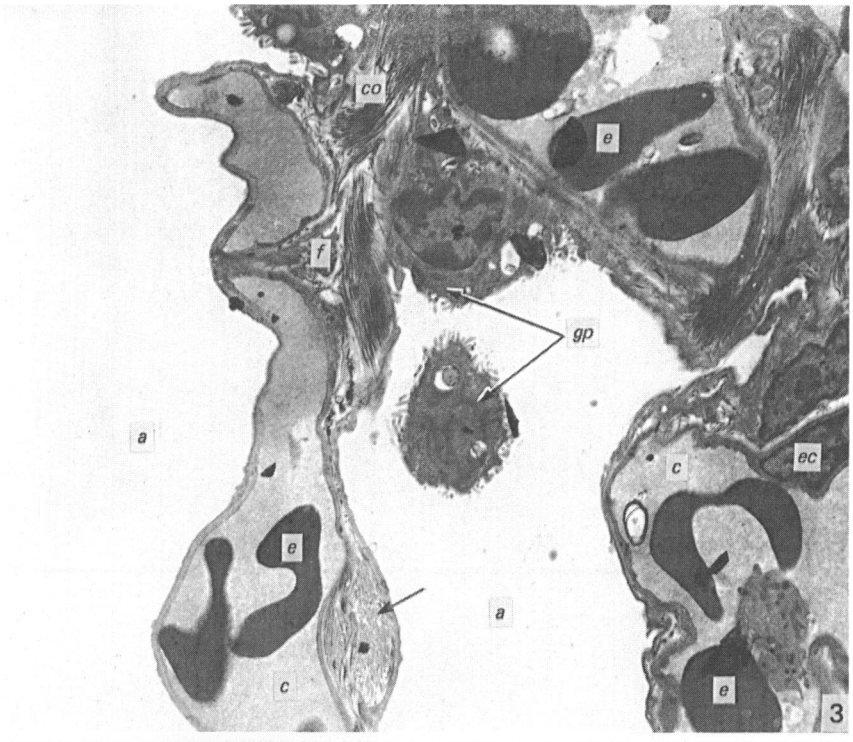

Figs. 3–4. Electron micrographs showing the components of the parenchyma. Collagen (*co*) is seen in the interstitium. Note the rare thickening of the blood–gas barrier in Figure 3 (arrow). *a*, alveoli; *c*, blood capillaries; *e*, erythrocyte; *gp*, granular pneumocyte; *ec*, endothelial cell; *ob*, osmiophilic body; *f*, fibrocyte. Figure 3 ×3300; Figure 4 ×10000.

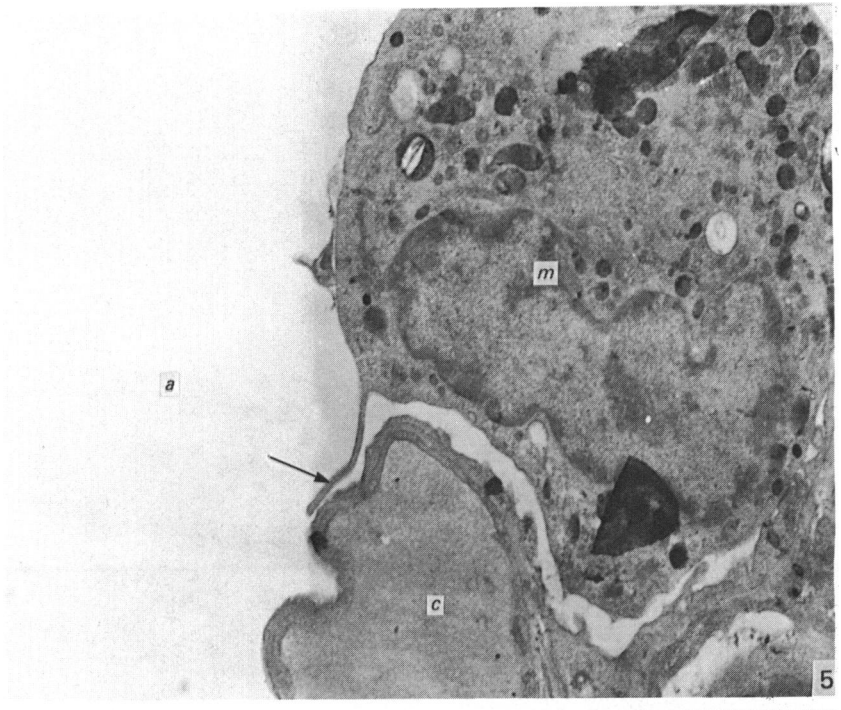

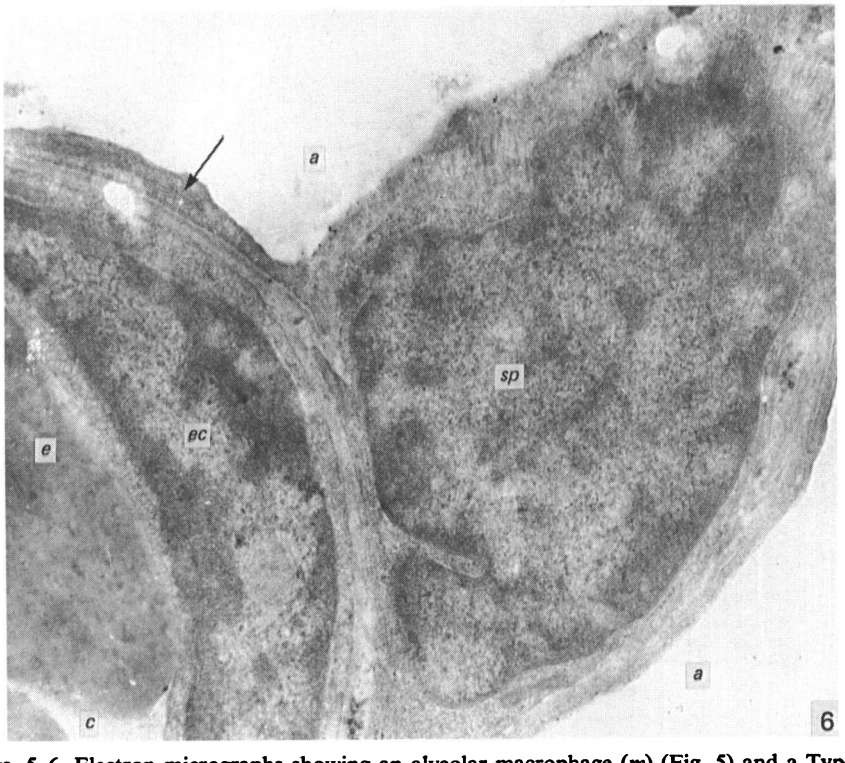

Figs. 5–6. Electron micrographs showing an alveolar macrophage (*m*) (Fig. 5) and a Type I (smooth) pneumocyte (*sp*) and an endothelial cell (*ec*) (Fig. 6). *a*, alveolus; *c*, blood capillary; *e*, erythrocyte. The arrow in Figure 5 shows a filopodia of a macrophage and that in Figure 6 a cytoplasmic flange of a Type I pneumocyte. Figure 5 × 6000; Figure 6 × 8600.

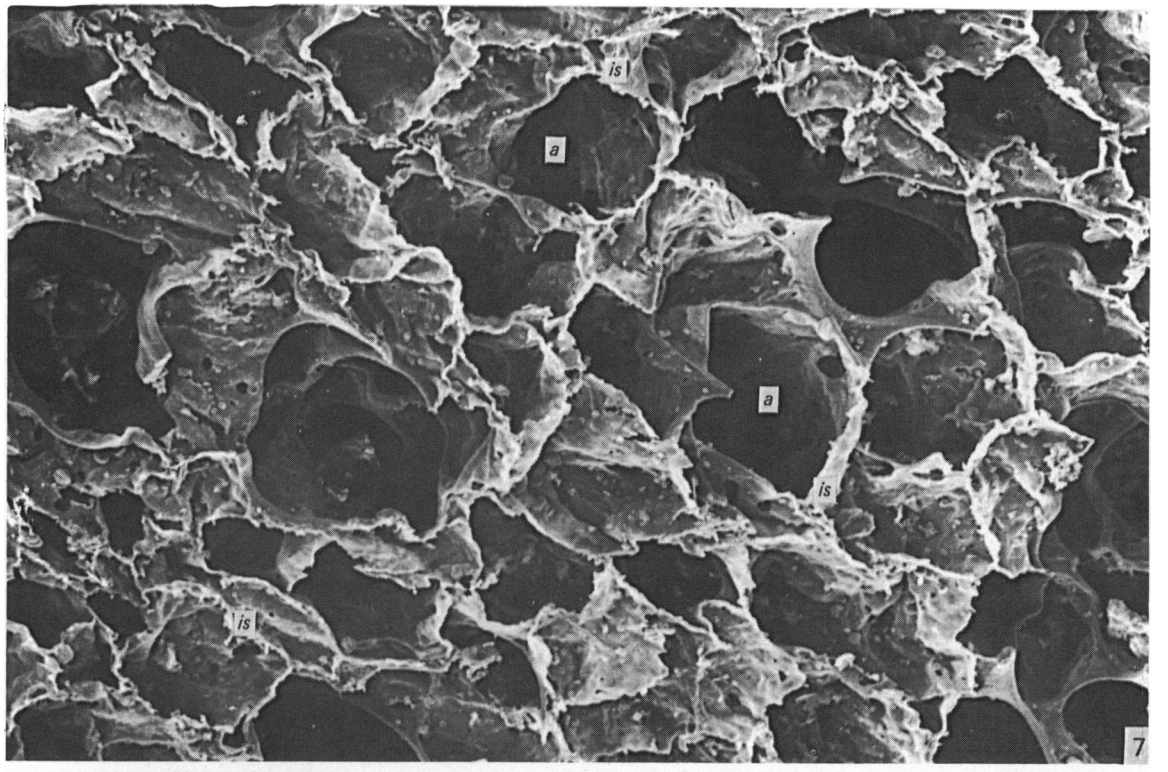

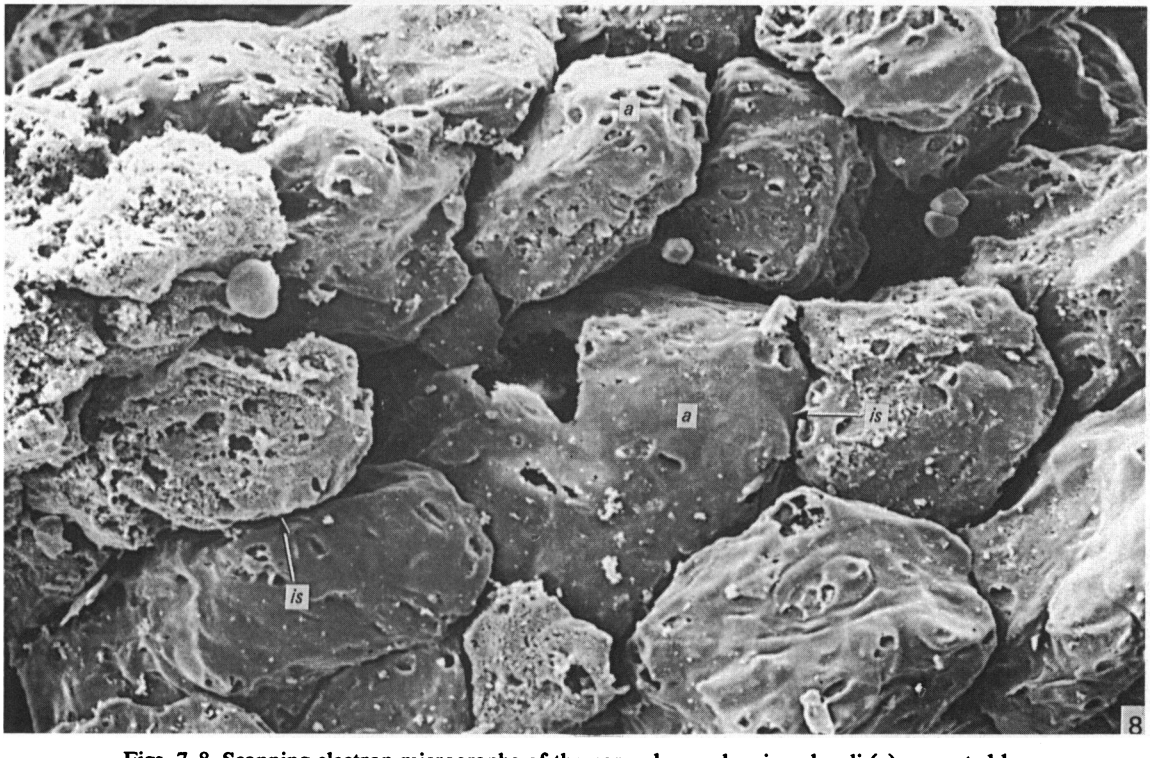

Figs. 7–8. Scanning electron micrographs of the parenchyma showing alveoli (*a*) separated by interalveolar septa (*is*). Figure 7 is a lung prepared by critical-point drying while Figure 8 is a latex cast preparation. The impressions on the alveoli (Fig. 7) could show areas occupied by the epithelial alveolar cells or, in some parts, are due to incomplete filling by the latex rubber. Figure 7 × 130; Figure 8 × 270.

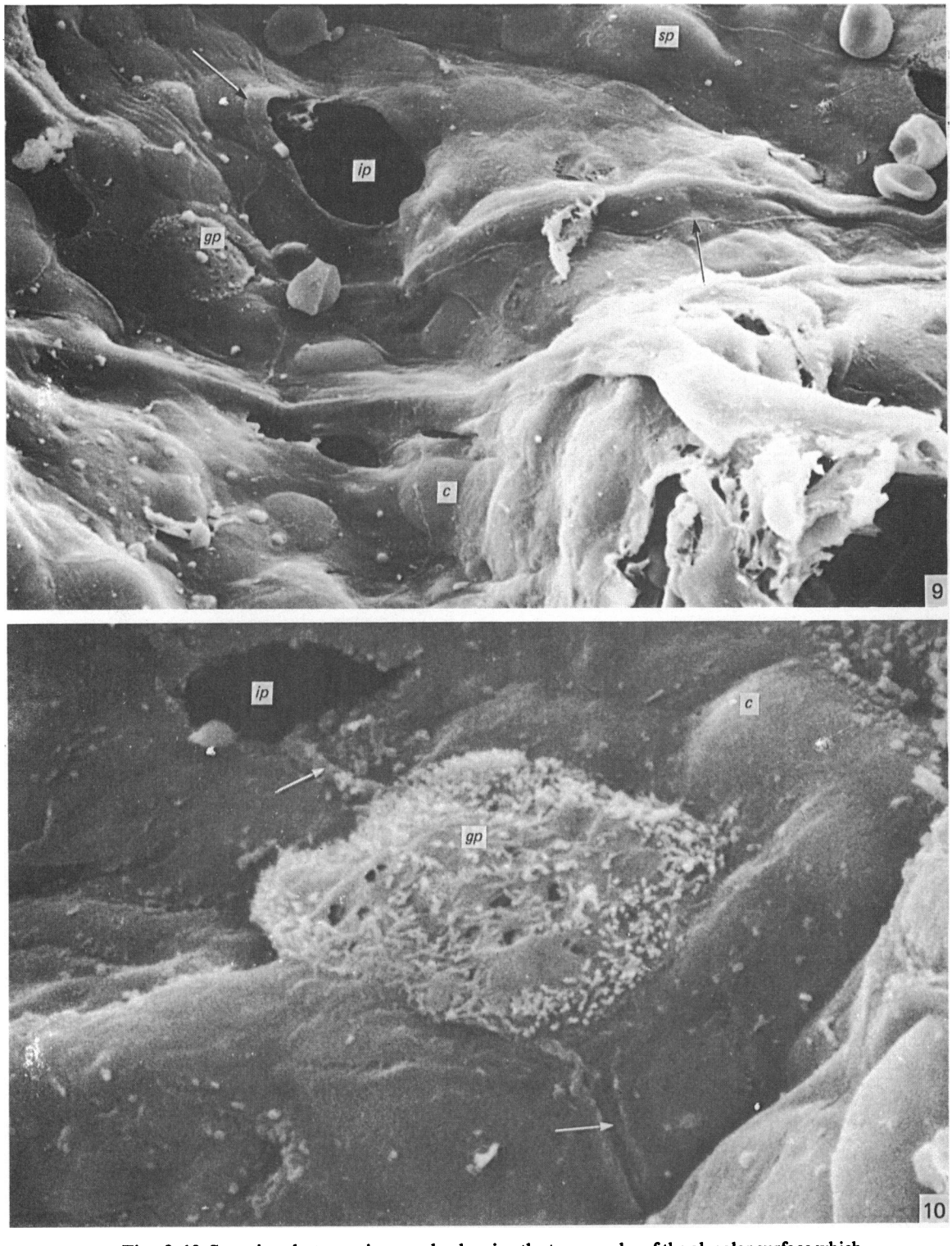

Figs. 9–10. Scanning electron micrographs showing the topography of the alveolar surface which is mainly made up of two populations of cells. The Type II (granular) pneumocytes (*gp*) and the Type I (smooth) pneumocyte (*sp*). *c*, a bulge of a blood capillary; *ip*, interalveolar pore. The arrows show the intercellular junctions of the alveolar cells. Figure 9 × 2000; Figure 10 × 7900.

Table 1. *Volume densities (%) and absolute volumes (cm^3) of the parenchyma and the non-parenchyma of the baboon lung*

Specimen	Body weight (kg)	Volume of the lung (V_L) (cm^3)	Parenchyma (p_a) (%)	Parenchyma (p_a) (cm^3)	Non-parenchyma (%)	Non-parenchyma (cm^3)
1	14·5	778	90·05	700·6	9·95	77·4
2	19·7	933	91·24	851·3	8·76	81·7
3	23·0	977	81·94	800·6	18·06	176·4
4	18·2	710	84·87	606·6	15·13	107·4
Mean	18·85	849·5	87·03	739·78	12·97	110·73
S.D.	3·53	126·22	4·37	108·64	4·37	45·74

Table 2. *Volume densities (%) and absolute volumes (cm^3) of the components of the parenchyma of the baboon lung*

Specimen	Alveoli (%)	Alveoli (cm^3)	Blood capillary (%)	Blood capillary (cm^3)	Interalveolar tissue (%)	Interalveolar tissue (cm^3)
1	77·44	542·2	8·72	61·10	13·84	97·0
2	73·89	629·03	10·03	85·99	16·08	136·28
3	76·38	611·5	6·65	53·24	16·97	135·86
4	78·00	470·03	5·26	31·66	16·74	100·91
Mean	76·42	563·27	7·67	58·00	15·91	117·51
S.D.	1·82	72·52	2·12	22·43	1·43	21·49

attenuated, had scattered micropinocytotic vesicles and was largely devoid of organelles (Figs. 2, 6). The preservation of the alveolar surface lining, the surfactant, was very poor in this study presumably as a result of most of it having been washed away after intracheal instillation with fixative. An interstitial space of varying thickness separated the alveolar epithelium from the endothelium. It contained ground substance and connective tissue elements such as collagen, fibrocytes, elastin and what occasionally appeared to be pericytes (Figs. 3, 4). The interstitial tissue elements were mainly encountered at the junctions between the blood capillaries and were scarce in the blood–gas (tissue) barrier itself. However, in a few cases (Fig. 3) collagen fibres were observed in the tissue barrier, such areas lying opposite very thin sections of the barrier. The endothelial cells, like the Type II pneumocytes, exhibited a notable degree of cytoplasmic extension from a centrally placed nucleus (Figs. 2, 6). The extensions exhibited sporadic attenuations and contained numerous micropinocytotic vesicles that were either free in the cytoplasm or continuous with the plasma membranes. On the alveolar surface occasional macrophages were observed (Fig. 5). These were large cells with a rather peripherally located nucleus, numerous mitochondria, diffuse lysosomal vesicles and filopodia for motility.

The results of the morphometric analysis are summarised in Tables 1–5. The parenchyma in the baboon lung formed, on average, 87 % of the lung, the remainder being contributed by the non-parenchymatous elements (Table 1). The alveoli, the blood capillaries and the tissues of the interalveolar septa respectively comprised 76, 8 and 16 % of the parenchyma (Table 2). The alveolar surface area exceeded those of the capillary endothelium, the blood–gas (tissue) barrier, and the red blood cell, while the area of the capillary endothelium in general exceeded both that of the

Table 3. *Surface areas of the alveoli (as), the capillary endothelium (ce), the blood–gas (tissue) barrier (tb) and the red-blood cell (rc)*

(The harmonic mean thicknesses of the tissue barrier (τh_t), that of the plasma layer (τh_p) and the arithmetic mean thickness of the tissue barrier (τ_t) are included.)

Specimen	*as* (m^2)	*ce* (m^2)	*tb* (m^2)	*rc* (m^2)	τh_t (μm)	τh_p (μm)	τ_t (μm)
1	101·98	79·56	71·09	52·22	0·323	0·240	0·941
2	123·79	86·42	73·38	86·0	0·530	0·260	1·51
3	104·46	73·23	65·10	32·99	0·500	0·140	1·03
4	99·36	66·14	60·55	88·19	0·560	0·170	0·979
Mean	107·40	76·34	67·53	64·85	0·478	0·203	1·12
S.D.	11·12	8·67	5·82	26·87	0·11	0·06	0·27

Table 4. *Anatomical pulmonary diffusing capacities for oxygen through the tissue barrier (D_{to_2}), plasma layer (D_{po_2})*, the red blood cell (D_{eo_2})*, the membrane (D_{mo_2})† and the overall diffusing capacity (D_{Lo_2})**

(The units are in $ml O_2$/min/mmHg.)

Specimen	D_{to_2}	D_{po_2} Min.	D_{po_2} Max.	D_{eo_2} Min.	D_{eo_2} Max.	D_{mo_2} Min.	D_{mo_2} Max.	D_{Lo_2} Min.	D_{Lo_2} Max.
1	726·20	879·53	1180·53	54·99	152·75	399·77	449·62	48·31	114·02
2	456·89	1061·05	1425·78	77·39	214·98	319·37	346·01	62·82	135·01
3	429·66	1215·31	1633·08	47·92	133·10	317·43	340·16	41·63	95·67
4	356·81	1452·61	1951·98	28·49	79·15	286·45	301·67	25·91	62·70
Mean	492·39	1152·24	1547·84	52·20	145·00	330·76	359·37	44·67	101·85
S.D.	161·50	242·76	326·81	20·19	56·08	48·42	63·30	15·32	30·65

* The maximum and minimum values were calculated from the relevant physical constants.
† D_{mo_2} and D_{Lo_2} are estimated from the relevant diffusing capacities.

tissue barrier and the red blood cells (Table 3). The harmonic mean thickness of the blood–gas (tissue) barrier in the specimens examined ranged from 0·323 to 0·560 μm (mean 0·478 μm ± 0·11 S.D.) while that of the plasma layer was notably smaller (0·140–0·260 μm) (Table 3). The arithmetic mean thickness of the blood–gas (tissue) barrier ranged from 0·941 to 1·51 μm (mean 1·12 μm ± 0·27 S.D.). The morphometric diffusing capacities of the barriers constituting the air-haemoglobin pathway are summarised in Table 4 and the weight specific values in Table 5. The mean morphometric diffusing capacity of the tissue barrier (D_{to_2}) was 492 ml O_2/min/mmHg while those of the plasma (D_{po_2}) and the red blood cell (D_{eo_2}) were 1350 and 99 ml O_2/min/mmHg respectively; the mean values for the membrane (D_{mo_2}) and the overall (total) morphometric diffusing capacity (D_{Lo_2}) were respectively 345 and 74 ml O_2/min/mmHg. The D_{mo_2} consistently exceeded the D_{Lo_2} due to the extra resistance that the red blood cell cytoplasm imposed on D_{Lo_2}, where oxygen biochemically reacts with the haemoglobin. The red blood cell contributed 77 % of the overall resistance offered by the air-haemoglobin pathway in the course of the diffusion of the oxygen molecules.

The mean weight specific volume of the lung was 0·046 cm^3/g and that of the surface area of the blood–gas (tissue) barrier 37 cm^2/g (Table 5). The mean surface density of the tissue barrier per unit volume of the parenchyma was 92 mm^2/mm^3

Table 5. *Some pulmonary morphometric ratios of the baboon, most of the values are normalised with body weight*

Specimen	V_L/W (cm^3/g)	S_{tb}/W (cm^2/g)	V_c/S_{tb} (cm^3/m^2)	S_{tb}/V_{pa} (mm^2/mm^3)	($ml O_2$/min/mmHg/kg) D_{tO_2}	D_{pO_2}*	D_{eO_2}*	D_{mO_2}*	D_{LO_2}*
1	0·054	49·03	0·86	101·47	50·08	71·04	7·16	29·29	5·60
2	0·047	37·25	1·17	86·20	38·42	63·12	7·42	16·89	5·02
3	0·042	28·30	0·82	81·31	18·68	61·92	3·94	14·3	2·98
4	0·039	33·27	0·52	99·82	19·60	93·53	2·96	16·16	2·43
Mean	0·046	36·96	0·84	92·20	31·70	72·40	5·37	19·16	4·01
S.D.	0·007	8·84	0·27	9·98	15·26	14·65	2·25	6·84	1·54

V_L, lung volume; W, body weight; V_{pa}, volume of the parenchyma; S_{tb}, surface area of the blood–gas (tissue) barrier; V_c, volume of the pulmonary capillary blood; D_{tO_2}, D_{pO_2}, D_{eO_2}, D_{mO_2} and D_{LO_2} are the diffusing capacities of the blood–gas (tissue) barrier, the plasma layer, the erythrocyte, the membrane and the total respectively.

* Mean values of the maximum and minimum values.

while the weight specific total morphometric pulmonary diffusing capacity was 4 ml O_2/min/mmHg/kg.

DISCUSSION

The gross, histological and ultrastructural organisation of the baboon lung was similar to that observed in the lungs of other primates (Kapanci *et al.* 1969; Kaplan *et al.* 1969; Davies & Reid, 1970; Greenwood & Holland, 1973; Castleman *et al.* 1975; Kerr *et al.* 1975; Gehr *et al.* 1978; Crapo *et al.* 1982; Tyler & Plopper, 1985), notably at the parenchymal level which was the main area of interest in the present investigation. The observations made here corroborate those made earlier by other workers (Castleman *et al.* 1975; Hislop *et al.* 1984; Wilson *et al.* 1984) namely that the lungs of the non-human primates are more representative as experimental models than those of the other subhuman mammals in studies related to the structure, development and presumably function and pathology of the human lung.

The parenchyma of the baboon lung, like that of a typical mammalian lung, was essentially made up of the alveoli, blood capillaries and the tissue of the interalveolar septum. The alveolar surface was made up of Type I and Type II pneumocytes. The Type I pneumocytes – the squamous cells – are said to cover 92 and 96 % of the alveolar surface in man and baboon respectively (Crapo *et al.* 1982; Burri 1985) and 96 % in the rat lung (Crapo, Barry, Foscue & Schelbourne, 1980). They may extend as much as 50 μm from the nucleus (Weibel, 1973). The squamous feature of the Type I alveolar cell has been considered a step towards optimising gas exchange (Burri, 1985). It is suggested here that this may also cut down on the alveolar cell number, hence reducing oxygen consumption by the lung tissue itself. On the alveolar surface the alveolar macrophage in man was observed to be the largest cell followed by the Type I cell and the Type II cell with the endothelial cell being the smallest in size (Crapo *et al.* 1982). However, in the same study it was found that the Type I cell constituted only 8 % of the parenchymal cell elements, the Type II cell contributing 16 %, with the remainder going to the endothelial cells (30 %), interstitial cells (36 %) and alveolar macrophages (9 %). The Type II cells were characterised by osmiophilic lamellated bodies which were presumed to be

precursors of the surfactant (Askin & Kuhn, 1971), and micropinocytotic vesicles which have been associated with transendothelial transport (Schneeberger & Karnovsky, 1968). Type III pneumocytes, or brush cells, as described by Meyrick & Reid (1968) in the rat lung and by Weibel (1973) in the dog were not observed in the baboon lung. In both *Papio* and *Homo* (Gehr *et al.* 1978) the blood–gas (tissue) barrier was essentially made up of an epithelium, an interstitium and an endothelium. The amount of interstitial connective tissue was distributed in such a way that a thick part of the barrier lay opposite a thin section of interstitial tissue. The thick parts are said to serve both for support and water exchange and thin ones for gas exchange (Fishman, 1972). The organisation of the connective tissue elements in the interalveolar septum, constituting a part of what has been termed the fibre continuum or the fibrous skeleton of the lung by Gehr *et al.* (1978), Weibel (1984) and Burri (1985), was interpreted as an attempt to attain an overall thin barrier without sacrificing its mechanical integrity. The large amount of the connective tissue, notably collagen, in the interalveolar septal tissue of the baboon lung was in part attributed to the advanced age of the specimens. However, an equivalent preponderance of the interalveolar connective tissue was observed in adult *Macaca irus* by Conradi *et al.* (1971) and in man by Gehr *et al.* (1978). In man the cellular elements constituted 50 % of the interstitium and were presumed to be involved in the regulation of the blood flow in the septum (Kapanci *et al.* 1974).

The design and structure of the lung in any given animal appears to reflect oxygen and metabolic demand which can be attributed to features such as body size and mode of life. Such structural characteristics in the lungs of a large number of terrestrial mammals have been elucidated by Gehr *et al.* (1981) in the bat (Maina & King, 1984) and in birds (Maina, 1984, 1987) by quantitative methods. Morphometric techniques, when correctly applied on biological materials, will yield representative data which could reveal possible interspecimen and interspecies differences. When the acquired data are applied to an appropriate model the cumulative functional effect of related morphometric parameters can be assessed.

The volume density of the parenchyma in the mammalian lungs appears to range from 80 to 90 % of the lung. In the horse this value was 86 % (Gehr & Erni, 1980) and in the wildebeest (*Connochaetes taurinus*) and the suni (*Nesotragus moschatus*) the values were 87 and 89 % respectively; in the six species of bat examined by Maina & King (1984) the values ranged from 83 to 85 %. The volume density of the parenchyma in the human lung (86·5 %) (Gehr *et al.* 1978) was closely similar to that of the baboon (87·03 %) found in this study. The value of 90 % proposed by Weibel (1963) for the average volume density of the parenchyma in the mammalian lung appears to be at the extreme upper end of the range. As the parenchyma constitutes an important reference space for the evaluation of the structural adaptation of the lung in gas exchange, the accuracy of its estimation influences that of the subsequently calculated values. It is suggested that the volume density of the parenchyma should be determined for every mammalian species and specimen under investigation in view of the apparent interspecimen differences in this parameter. The mean volume densities of the components of the parenchyma – the alveoli, the blood capillaries and the tissue of the interalveolar septum – in the human specimens examined by Gehr *et al.* (1978) were respectively 86·5, 5·7 and 7·8 %, while those reported by Kapanci & Tosco (1972) were correspondingly 82, 6·1 and 13 %; the equivalent values for the baboon lung were respectively 76·4, 7·7 and 15·9 % (Table 2). In the rhesus monkey (*Macaca mulatta*) (Kapanci *et al.* 1969), the tissue of the interalveolar septum

Table 6. *Comparison of some morphometric values of the primate lung*. (Some of the parameters have been normalised with body weight (W). The symbols are defined in Tables 3, 4 and 5.)*

Source of the data: *Papio*, this study; *M. irus*, Conradi *et al.* (1971) – values taken from Weibel (1973). Table 2; *M. mulatta*, Kapanci *et al.* (1969). *H. sapiens*, Gehr, Bachofen & Weibel (1978).

* Some of the values were calculated from the given data where the actual required value was not available.

	V_L/W (cm³/kg)	S_{tb}/W (cm²/g)	S_{tb}/V_{pa} (mm²/mm³)	S_{ce}/V_L (m²/cm³)	V_c/S_{tb} (cm³/m²)	V_c/V_L (cm³/cm³)	V_c/W (cm³/kg)	τht (μm)	(ml O_2/min/mmHg/kg) D_{tO_2}/W	(ml O_2/min/mmHg/kg) D_{LO_2}/W
Papio anubis	46	37	92	0·090	0·84	0·068	3·08	0·478	32	4 [5·4]†
Macaca irus	50	33	76	0·065	1·20	0·081	4·04	0·500	22	– [6·5]†
Macaca mulatta	—	—	—	0·058	—	0·067	—	—	—	—
Homo sapiens	59	18	35	0·029	1·58	0·057	2·88	0·620	10	2·6 [3·6]†

† The values in brackets are maximum total morphometric pulmonary diffusing capacities and those not in brackets body weight normalised values of the mean D_{LO_2}.

comprised 15 % of the parenchyma. In the lungs of the other mammalian species that have been examined, these values were 78·05, 11·09 and 10·89 % in the shrew (Gehr *et al.* 1980) and 82, 9·2 and 8·8 % in the horse (Gehr & Erni, 1980). The data currently available indicates that the volume density of the blood capillaries tends not to vary a great deal, the changes in the composition of the parenchyma largely involving the alveoli and the tissue of the interalveolar septum. This could suggest that of the two structural features of the parenchyma, the pulmonary capillary blood rather than the alveolar surface area may be the more significant limiting factor in gas exchange. Alveolar size dependency observed in the dog lung by Glazier, Hughes, Maloney & West (1967) and in the horse lung by Gehr & Erni (1980) was not apparent in the baboon lung; in the human lung, regional variation in the alveolar size was not observed (Gehr *et al.* 1978).

In this study a comparison has been made between the morphometric characteristics of the parameters involved in gas exchange in the lungs of the primates (Table 6) as far as the data allow. It is apparent that the human lung is structurally less well adapted for gas exchange than that of the non-human primate. The weight specific surface area for gas exchange in *Papio anubis* (37 cm²/g) and in *Macaca irus* (34 cm²/g) was about twice that in *Homo sapiens* (18 cm²/g). Concerning the volume of the pulmonary capillary blood per unit surface area of the blood–gas (tissue) barrier (Vc/Stb), the capillary loading, in *Homo* (1·58 cm³/m²) was almost twice that in *Papio* (0·84 cm³/m²) and notably higher than in *Macaca irus* (1·2 cm³/m²). Capillary loading indicates the degree of exposure of the pulmonary capillary blood to alveolar air (Perry, 1978), a relatively high value in *Homo* suggesting a poor degree of exposure. The harmonic mean thickness which is the most meaningful parameter in assessing a barrier resistance to oxygen diffusion (Weibel, 1970/71) was thinner in *Papio* (0·478 μm) than in *Macaca irus* (0·500 μm) and thickest in *Homo* (0·620 μm). The harmonic mean thickness of the blood gas (tissue) barrier in *Papio* falls within the range of 0·26 μm in the shrew to 0·62 μm in man (Gehr *et al.* 1981). The arithmetic mean thickness in *Papio* (1·12 μm) was remarkably smaller than in *Homo* (2·2 μm) (Table 6). The ratio of the arithmetic to harmonic mean thickness is said to

Table 7. *Comparison of pulmonary morphometric parameters of a non-human primate and a non-primate mammal of comparable body weight and a bird*

(Symbols defined in Tables 2, 4 and 5)

Sources of data: *Papio*, this study; *Gazella*, Gehr *et al.* (1981); *Adeotis*, Maina (unpublished data).

	Common English names	W (kg)	V_L (cm^3)	S_{tb} (m^2)	τht (μm)	V_c (cm^3)	D_{LO_2}* (ml O_2/min/mmHg/kg)
Papio anubis	Olive baboon	19	850	68	0·478	58	73
Gazella thomsoni	Thomson's gazelle	20	1670	87	0·380	119	129
Adeotis kori	Kori bustard	13	336	26	0·203	40	39

* D_{LO_2}, mean of the maximum and minimum values.

reflect the corrugation or the sporadic attenuation of the blood–gas (tissue) barrier (Weibel & Knight, 1964; Meban, 1980), a higher ratio suggesting a greater degree of corrugation. The ratio in man of 3·6 (Gehr *et al.* 1978) was higher than in *Papio* (2·3). Sporadic attenuation of the barrier is said to be advantageous as it enhances gas exchange by attaining an overall thinner barrier without sacrificing its mechanical and functional integrity (Weibel & Knight, 1964).

The maximum weight-specific total morphometric pulmonary diffusing capacity in *Homo sapiens* (3·6 ml O_2/min/mmHg/kg) was notably lower than in *Macaca irus* (6·5) and *Papio anubis* (5·4). This feature is a reflection of the more extensive surface areas, thinner blood–gas (tissue) barrier and the higher pulmonary capillary blood volume in *Papio* and *Macaca* (Table 6), these three features directly determining the overall pulmonary diffusing capacity. The human values for the alveolar surface area and the total morphometric pulmonary diffusing capacity fell below the common regression line and tended to conform to those of the less active 'captive' animals in the population of animals examined by Weibel (1972) and Gehr *et al.* (1978). This indicates that the human lung is structurally less well adapted for gas exchange when compared with the lungs of the wild, agile mammals. The lungs of *Macaca irus* (Conradi *et al.* 1971) appear to be morphometrically better adapted for gas exchange than those of *Papio*, with the maximum total morphometric pulmonary diffusing capacity being 20 % higher in the macaque. The rhesus monkey is smaller than the baboon and presumably is more active.

The small size of the macaque would lead to a higher resting metabolic rate which accounts for the better pulmonary gas exchange adaptations in this species. The morphometric features of *Papio* (Table 7) were less specialised than those of the Thomson's gazelle (*Gazella thomsoni*) (Gehr *et al.* 1981), an energetic mammal of equivalent body weight which lives in the open savanna and is constantly on the move to escape from predators.

This study clearly indicates that there is a pressing need to examine the lungs of more non-human primates, particularly those of the apes. The anthropoid apes are known to be closer to man than the monkeys (Clark, 1970). The knowledge gained from such studies could be invaluable in the preservation of the primates, and particularly in related biomedical research.

SUMMARY

The gross, histological and ultrastructural organisation of the baboon lung was found to be similar to that of the human lung. It is suggested that, in general, the lungs of the non-human primates would serve as ideal models for the study of the human lung.

The baboon lung comprises the parenchyma, the gas exchange part of the lung which consists of alveoli, blood capillaries and the tissue of the interalveolar septum, and the non-parenchyma made up of the air conducting passages like bronchi, bronchioles, larger blood vessels, connective tissue and pleura. On morphometric analysis, the parenchyma was found to constitute 87 % of the lung, the rest being made up of the elements of the non-parenchyma. The alveoli, blood capillaries and the interalveolar tissue respectively constituted 76, 8 and 16 % of the parenchyma.

The harmonic mean thickness of the blood–gas (tissue) barrier was 0·475 μm and the arithmetic mean 1·12 μm, the ratio being 1:2·3. The weight specific surface area of the blood–gas (tissue) barrier was 37 cm^2/g and the surface density of the tissue barrier in the parenchyma 92 mm^2/mm^3. The total morphometric pulmonary diffusion per unit body weight was 4 ml O_2/min/mmHg/kg and the volume of the pulmonary capillary blood per unit surface area of the tissue barrier 0·84 cm^3/m^2.

Morphometrically the baboon lung was thus observed to be better adapted for gas exchange than that of man but less specialised than that of the smaller monkeys such as *Macaca mulatta*.

I gratefully acknowledge the help received from various individuals and institutions without whose aid this work would not have been possible. I thank Dr J. Else, the Director of the Institute of Primate Research, National Museums of Kenya, Nairobi, for making it possible for me to acquire the baboon lungs. The use of the TEM was made possible through the courtesy of Professor G. M. Mugera, Head of the Department of Pathology and Microbiology, University of Nairobi. The SEM part of this work was carried out at the Anatomical Institute, University of Bern, Switzerland. I thank Professor E. R. Weibel, the Director of the Institute for kindly allowing me to use the facilities and Dr P. Gehr and Mr K. Babl for numerous courtesies. The immense help given to me by Professor A. S. King during the formative stages of my studies in pulmonary morphometry is highly appreciated. I am indebted to the Leverhulme Trust of London for their generous financial help in this and other studies.

REFERENCES

ASKIN, F. B. & KUHN, C. (1971). The cellular origin of pulmonary surfactant. *Laboratory Investigation* **25**, 260–268.

BOURNE, G. H. (1973). The primate research centre program of the National Institute of Health. In *Non Human Primates and Medical Research* (ed. G. H. Bourne), pp. 487–513. New York, London: Academic Press.

BOYDEN, E. A. (1977). The development of the lung in the pigtail monkey (*Macaca nemestrina*, L). *Anatomical Record* **186**, 15–38.

BREEZE, R. G. & WHEELDON, E. B. (1977). The cells of the pulmonary airways. *American Review of Respiratory Disease* **116**, 705–777.

BROWN, L. S., BLISS, A. S. & LONGMORE, W. J. (1984). Effect of nutritional status on the lung surfactant system: food deprivation and caloric restriction. *Experimental Lung Research* **6**, 133–147.

BURRI, P. H. (1985). Morphology and respiratory function of the alveolar unit. *International Archives of Allergy and Applied Immunology* **76**, 2–12.

CARSTENS, L. A. & ALLEN, J. R. (1969). Ultrastructural modifications in the lungs of the fetal rhesus monkey. *Journal of Cell Biology* **43**, 17A.

CASTLEMAN, W. L., DUNGWORTH, D. L. & TYLER, W. S. (1975). Intrapulmonary airway morphology in three species of monkeys: A correlated scanning and transmission electron microscopic study. *American Journal of Anatomy* **142**, 107–122.

CLARK, W. E. LE GROS (1970). *History of the Primates*. London: Staples.

CONRADI, C., BURRI, P. H., KAPANCI, Y., ROBINSON, F. R. & WEIBEL, E. R. (1971). Lung changes after beryllium inhalation. *Archives of Environmental Health* **23**, 346–358.

CRAPO, J. D., BARRY, B. E., GEHR, P., BACHOFEN, M. & WEIBEL, E. R. (1982). Cell numbers and cell characteristics of the normal human lung. *American Review of Respiratory Diseases* **125**, 332–337.

CRAPO, J. D., BARRY, B. E., FOSCUE, H. E. & SCHELBOURNE, J. S. (1980). Structural and biochemical changes in rat lungs occurring during exposures to lethal and adaptive doses of oxygen. *American Review of Respiratory Diseases* **122**, 123–145.

DAVIES, G. M. & REID, L. (1970). Growth of the alveoli and pulmonary arteries in childhood. *Thorax* **25**, 669–681.

FISHMAN, A. P. (1972). Pulmonary edema: The water exchanging function of the lung. *Circulation* **46**, 390–408.

GEHR, P. (1984). Respiratory tract structure and function. In *Fundamentals of Extrapolation Modeling of Inhaled Toxicants* (ed. F. J. Miller), pp. 236–249. New York, London: Hemisphere Publishing Co.

GEHR, P., BACHOFEN, M. & WEIBEL, E. R. (1978). The normal human lung: Ultrastructure and morphometric estimation of diffusion capacity. *Respiration Physiology* **32**, 121–140.

GEHR, R. & ERNI, H. (1980). Morphometric estimation of pulmonary diffusion capacity in two horse lungs. *Respiration Physiology* **41**, 199–210.

GEHR, P., MWANGI, D. K., AMMANN, A., MALOIY, G. O. M., TAYLOR, C. R. & WEIBEL, E. R. (1981). Design of the mammalian respiratory system. V. Scaling morphometric pulmonary diffusing capacity to body mass: Wild and domestic mammals. *Respiration Physiology* **44**, 61–86.

GEHR, P., SEHOVIC, S., BURRI, P. H., CLAASSEN, H. & WEIBEL, E. R. (1980). The shrew lung: morphometric estimation of diffusion capacity. *Respiration Physiology* **40**, 33–47.

GLAZIER, J. E., HUGHES, J. M. B., MALONEY, J. E. & WEST, J. B. (1967). Vertical gradient of alveolar size in lungs of dogs frozen intact. *Journal of Applied Physiology* **23**, 694–705.

GREENWOOD, M. F. & HOLLAND, P. (1973). Scanning electron microscopy of the normal and BCG-stimulated primate respiratory tract. *Journal of the Reticulo-endothelial Society* **13**, 183–192.

GRANT, M. M., SOROKIN, S. P. & BRAIN, J. D. (1979). Lysosomal enzyme activities in pulmonary macrophages from rabbits breathing iron oxide. *American Review of Respiratory Diseases* **120**, 1003–1012.

HIRAI, K., UYEDA, T. & OGAWA, K. (1984). Electron cytochemical studies on the differentiation of mouse lung alveolar epithelial cells with special references to changes in mitochondria. *Acta histochemica et cytochemica* **17**, 197–211.

HISLOP, A., HOWARD, S. & FAIRWEATHER, D. V. I. (1984). Morphometric studies on the structural development of the lung in *Macaca fasciculata* during fetal and postnatal life. *Journal of Anatomy* **138**, 95–112.

KAPANCI, Y., ASSIMACOPOULOS, A., IRLE, C., SWAHLEM, A. & GABBIANI, G. (1974). Contractile interstitial cell in pulmonary alveolar septa: A possible regulator of ventilation/perfusion ratio? *Journal of Cell Biology* **60**, 375–392.

KAPANCI, Y. & TOSCO, R. (1972). Oxygen pneumonitis in man, light and electron microscopic morphometric studies. *Chest* **62**, 162–169.

KAPANCI, Y., WEIBEL, E. R., KAPLAN, H. P. & ROBINSON, F. R. (1969). Pathogenesis and reversibility of the pulmonary lesions of oxygen toxicity in monkeys. II. Ultrastructural and morphometric studies. *Laboratory Investigation* **20**, 101–118.

KAPLAN, H. P., ROBINSON, F. R., KAPANCI, Y. & WEIBEL, E. R. (1969). Pathogenesis and reversibility of the pulmonary lesions of oxygen toxicity in monkeys I. Clinical and light microscopic studies. *Laboratory Investigation* **20**, 94–100.

KERR, G. R., COUTURE, J. & ALLEN, J. R. (1975). Growth and development of the fetal rhesus monkey. VI. Morphometric analysis of the developing lung. *Growth* **39**, 67–84.

KERR, G. R. & HELMUTH, A. C. (1974). Growth and development of the fetal rhesus monkey. V. Fatty acids of phospholipids in fetal lung. *Biology of the Neonate* **25**, 10–22.

LAPIN, B. A. (1971). Use of primates in biomedical research. In *The Use of Non-human Primates in Research on Human Reproduction* (ed. E. Diczfalusy & C. C. Standley), pp. 15–17. Stockholm: Karolinska Sjukhuset.

LECHNER, A. J. (1985). Pulmonary design in a microchiropteran bat (*Pipistrellus subflavus*) during hibernation. *Respiration Physiology* **59**, 301–312.

MAINA, J. N. (1984). Morphometrics of the avian lung. 3. The structural design of the passerine lung. *Respiration Physiology* **55**, 291–307.

MAINA, J. N. (1985). A scanning and transmission electron microscope study of the bat lung. *Journal of Zoology* **205A**, 19–27.

MAINA, J. N. (1987). The morphometry (quantitative anatomy) of the avian lung. In *Form and Function in Birds*, vol. IV (ed. A. S. King & J. McLelland). London: Academic Press (In the Press.)

MAINA, J. N. & KING, A. S. (1984). Correlation between structure and function in the design of the bat lung: A morphometric study. *Journal of Experimental Biology* **111**, 43–61.

MEBAN, C. (1980). Thickness of the air–blood barriers in vertebrate lungs. *Journal of Anatomy* **131**, 299–307.

MEYRICK, B. & REID, L. (1968). The alveolar brush cells in the rat lung – a third pneumocyte. *Journal of Ultrastructure Research* **23**, 71–82.

PERRY, S. F. (1978). Quantitative anatomy of the lungs of the red-eared turtle *Pseudemys scripta elegans*. *Respiration Physiology* **35**, 245–262.

PINKERTON, K. E., BARRY, B. E., O'NEIL, J., RAUB, J. A., PRATT, P. C. & CRAPO, J. D. (1982). Morphological changes in the lung during the lifespan of Fisher 344 rats. *American Journal of Anatomy* **164**, 155–174.

SCHNEEBERGER, E. E. & KARNOVSKY, M. J. (1968). The ultrastructural basis of alveolar capillary membrane permeability to peroxidase used as a tracer. *Journal of Cell Biology* **37**, 781–793.

SOROKIN, S. P. & BRAIN, J. D. (1975). Pathways of clearance in mouse lungs exposed to iron oxide aerosols. *Anatomical Record* **181**, 581–626.

THURLBECK, W. M. (1982). Postnatal human lung growth. *Thorax* **37**, 564–571.

TYLER, N. K. & PLOPPER, C. G. (1985). Morphology of the distal conducting airways in rhesus monkey lungs. *Anatomical Record* **211**, 295–303.

WANG, N. S. & THURLBECK, W. M. (1970). Scanning electron microscopy of the lung. *Human Pathology* **1**, 227–337.

WEIBEL, E. R. (1963). *Morphometry of the Human Lung*. Berlin: Springer Verlag.

WEIBEL, E. R. (1970/71). Morphometric estimation of pulmonary diffusion capacity. I. Model and method. *Respiration Physiology* **11**, 54–75.

WEIBEL, E. R. (1972). Morphometric estimation of pulmonary diffusion capacity. V. Comparative morphometry of alveolar lungs. *Respiration Physiology* **41**, 26–63.

WEIBEL, E. R. (1973). Morphological basis of alveolar-capillary gas exchange. *Physiological Reviews* **53**, 419–491.

WEIBEL, E. R. (1979). *Stereological Methods*, vol. 1. *Practical Methods for Biological Morphometry*. London: Academic Press.

WEIBEL, E. R. (1984). *The Pathway for Oxygen: Structure and Function in the Mammalian Respiratory System*. Cambridge, Mass.: Harvard University Press.

WEIBEL, E. R. & GIL, J. (1977). Structure–function relationships at the alveolar level. In *Bioengineering Aspects of the Lung* (ed. J. B. West), pp. 1–81. New York: Marcel Dekker.

WEIBEL, E. R. & KNIGHT, B. (1964). A morphometric study on the thickness of the pulmonary air–blood barrier. *Journal of Cell Biology* **21**, 367–384.

WILSON, D. W., PLOPPER, C. G. & HYDE, D. M. (1984). The tracheobronchial epithelium of the bonnet monkey *Macaca radiata*; quantitative ultrastructural study. *American Journal of Anatomy* **171**, 25–40.

WINKLER, G. C. & CHEVILLE, N. F. (1985). Morphometry of the postnatal development in the porcine lung. *Anatomical Record* **211**, 427–433.